textiles

MDPI

Article

Radical and Catalyst Effect on Fenton-like Textile Dyes' Degradation Process and Techno-Economical Consideration

Guntur Adisurya Ismail [1,2] and Hiroshi Sakai [2,*]

[1] Department of Chemical Engineering, Faculty of Industrial Technology, Bandung Institute of Technology, Ganesha Str. No. 8, Bandung 40132, West Java, Indonesia; guntur.adisurya@itb.ac.id
[2] Department of Civil and Environmental Engineering, School of Urban and Environmental Sciences, Tokyo Metropolitan University, 1–1 Minami-Osawa, Hachioji-City 192-0397, Tokyo, Japan
* Correspondence: h_sakai@tmu.ac.jp

Abstract

This study investigates Fenton-based processes for textile dye degradation, focusing on Direct Red 28 (DR28), Reactive Blue 19 (RB19), and Reactive Black 5 (RBk5). Results reveal varying effectiveness of catalyst–radical combinations, with copper and peroxydisulfate consistently performing well, especially on RBk5 with 100% and 98.5% decolorization and total organic carbon (TOC) reduction, respectively. Iron faces limitations with DR28 due to sediment formation, resulting in 3.5% and 52.7% TOC removal when paired with hydroxyl and peroxydisulfate radicals, correspondingly. Unexpectedly, cobalt shows notable capabilities with RBk5, reaching 87.2% TOC removal, but performs poorly on the other two dyes, with less than 20% TOC removal when paired with hydroxyl radicals. Cost analysis highlights the cost-effectiveness of the standard photo-Fenton process for easy-to-degrade dyes with a cost of $0.174/g TOC removed, while copper emerges as a viable option for recalcitrant dyes, costing $0.371/g TOC removed. Overall, this research enhances understanding of catalyst–radical interactions on various dyes, a topic that is scarcely discussed in other research, and expands upon it by using techno-economic analysis for Fenton-based technologies for textile wastewater treatment, as a consideration for technology selection in actual application.

Keywords: Fenton; decolorization; hydroxyl radicals; sulfate; cost

check for updates

Academic Editor: Laurent Dufossé

Received: 4 July 2025
Revised: 21 August 2025
Accepted: 26 August 2025
Published: 1 September 2025

Citation: Ismail, G.A.; Sakai, H. Radical and Catalyst Effect on Fenton-like Textile Dyes' Degradation Process and Techno-Economical Consideration. *Textiles* **2025**, *5*, 37. https://doi.org/10.3390/textiles5030037

Copyright: © 2025 by the authors. Licensee MDPI, Basel, Switzerland. This article is an open access article distributed under the terms and conditions of the Creative Commons Attribution (CC BY) license (https://creativecommons.org/licenses/by/4.0/).

1. Introduction

The treatment of recalcitrant water pollutants has been a major topic of discussion in recent years, particularly the removal of dyestuff compound from textile wastewater. With the rapid development of the fashion industry, environmental issues related to water quality arise, especially for the color. Color has received increasing attention, mainly due to its offensive appearance in the environment [1].

The Fenton process for pollutant degradation has been studied since 1876 and has further developed into various Fenton-based processes; it has seen actual implementation and is even considered to be the best technology to remove emerging pollutants [2,3]. Fenton-based processes are also used in textile wastewater treatment [4]. Textile wastewater typically contains high chemical oxygen demand (COD), total solids (TS) and, more importantly, obnoxious color [5]. In actual textile wastewater treatment plants, the removal of TS and COD can be performed by employing sedimentation and the biological process, respectively. However, these processes are not capable of removing color to an acceptable

level. Color removal is usually performed via coagulation-flocculation, which takes place after the biological process. However, this process produces sediment that requires further handling. There are also cases where the color returns to its initial condition after being discharged to the environment [6]. The issue became much more important with the inclusion of color as an effluent standard, urging the need for alternative processes that could degrade color safely and efficiently [7].

The application of Fenton-based processes to textile dye degradation has been extensively investigated with mostly positive results [8–11]. However, research on the direct comparison of various Fenton-based processes on different textile dyes is still uncommon. In actual treatment plants, not only one but several types of dyed wastewater should be treated. From this perspective, it is important to compare the treatment efficiency of multiple types of wastewaters by the Fenton-based process for plant design.

To the best of the author's knowledge, there is no comparative study on the combination of different catalysts, radicals, and textile dyes. Dyes are organic compounds containing functional groups and chromophores. Their degradation is evaluated by decolorization or reduction of total organic carbon (TOC), which is strongly influenced by the type of catalyst and radical agent, resulting in different treatment costs. Our previous finding [12] also showed that sediment may be formed during dye degradation due to a complex reaction between dyes and the catalyst, which also affects the complexity of treatment and finally the total cost. Thus, this research is conducted to provide insight and discussion on how different combinations of catalysts and radical agents could affect the degradation performance of various textile dyes, and how it may affect the complexity of treatment, which will also affect the cost of treatment.

2. Materials and Methods

Direct red 28 (DR28, ≥80%), hydrogen peroxide (H_2O_2, 30–35%), potassium peroxydisulfate (PDS) ($K_2S_2O_8$, ≥99%), iron (II) sulfate heptahydrate ($FeSO_4 \cdot 7H_2O$, ≥99%), cobalt (II) heptahydrate ($CoSO_4 \cdot 7H_2O$, ≥99%), sodium hydroxide (NaOH, ≥97%) and sulfuric acid (H_2SO_4, ≥96) were purchased from Kanto Chemical co., inc, while reactive blue 19 (RB19, 40–65%) and reactive black 5 (RBk5, ≥50%) were obtained from Sigma-Aldrich and copper (II) sulfate pentahydrate ($CuSO_4 \cdot 5H_2O$, ≥99.5%) was purchased from Hikotaro Tsudzui co. ltd (now Kanto Chemical, Tokyo, Japan). All chemicals were used as received without prior purification.

These dyes were selected because of their widespread use in the textile industry or as representatives of a particular dye group. DR28 (also known as Congo Red) was the first non-mordant direct dye to be marketed and it even influenced the development of other "Congo" named-dyes. It was first found in Germany, and still sees significant usage, despite being banned in several countries in Europe due to the toxic benzidine that acts as the dye's backbone [13]. DR28 has also found an application outside the textile sector, for amyloid staining [14]. RBk5 is the most commonly used reactive dye in the finishing of cotton, wool, and nylon [15]. RB19 is the most popular anthraquinone dye, despite its low fixation efficiency (75–80%) to the fiber compared to other reactive dyes [16]. However, we found that this dye is widely available in local markets in Indonesia and is often used to dye jeans.

Synthetic dye wastewater was prepared by dissolving 350 mg of specific dyes in 3.5 L of ultrapure water, resulting in a dye concentration of 100 mg/L, representing the typical dye concentrations found in real wastewater [17,18]. It should be noted, however, that increasing the dye's concentration will reduce the removal efficiency, due to limited radical availability and the difficulties of the radical to penetrate the more saturated dye's compound [19,20]. The prepared dye solution was continuously stirred in a stainless

steel reservoir, equipped with a 254 nm UV lamp (QGL8W-21, Iwasaki Electric, Tokyo, Japan), with affluence of 5.94 mW/cm^2 at the surface and center of the lamp. The pH of the solution was adjusted using 1 M NaOH solution or concentrated H_2SO_4. While the standard Fenton process is commonly performed in a pH of 3, textile wastewater is commonly a neutral pH or even alkaline (pH > 10) due to the usage of caustic during the process [21]. A combination of 10 mM of the radical source and 0.5 mM of the metal catalyst was added to the system for each dye, resulting in 54 total run variations, as shown in the variations depicted in Figure 1. Six more variations which involve no metal catalyst were also performed, resulting in a total of 60 run variations. Samples were collected at various time points, including 0 min (before any chemical addition) and after 15, 30, 60, and 90 min. In addition, a portion of the samples was filtered through a 0.45 µm filter for comparison and subjected to similar analyses.

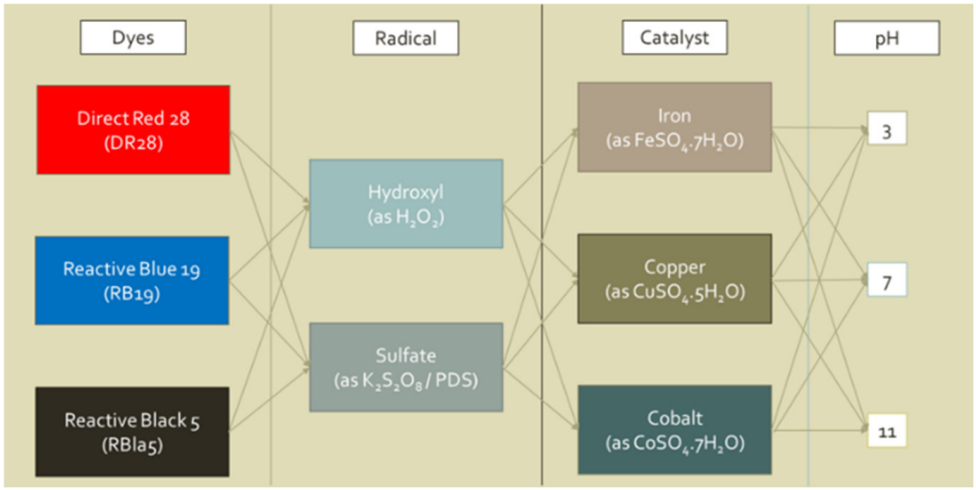

Figure 1. Variation used in this experiment.

Two analytical procedures were employed in this study. The first analysis involved spectral absorbance analysis, which measured the reduction in dye absorbance at their respective optimum wavelengths. Spectral absorbance measurements were conducted using a spectrophotometer (Jasco, Tokyo, Japan. V-670 UV-Vis-NIR spectrophotometer) by assessing the absorbance of the sample over a wavelength range of 200–800 nm. In addition, TOC was measured to evaluate the extent of dye degradation after treatment. Samples were stored in a 4 °C refrigerator in a glass beaker covered with aluminum foil prior to TOC analysis. TOC analysis was performed using a TOC analyzer (Shimadzu, Kyoto, Japan. TOC-VCSH). All samples were thoroughly mixed before analysis.

Cost calculation was performed by using the cost reference shown in Table 1. Pricing information was obtained from the e-commerce marketplace IndiaMart (accessed on 30 October 2024). While some references have suggested potentially higher prices for individual chemicals, particularly peroxide, peroxydisulfate, and iron sulfate [22–24], there is a relative paucity of cost assessments for copper and cobalt catalysts in Fenton-like systems. The cost references provided in Table 1 are close to those found in other studies using similar conditions [25–27]. As can be seen, the range of electricity consumption between the different references is quite wide, so the median value will be used for the calculation.

Table 1. Cost breakdown.

Component	Usage	Price	Cost (Per m^3)	Reference
H_2O_2/H	1 L/m^3	\$0.962/L	0.962 \$	Current work, [22]
$K_2S_2O_8$/PDS	2.7 kg/m^3	\$1.804/L	4.870 \$	Current work, [24]
$FeSO_4$	139 g/m^3	\$1.022/kg	0.142 \$	Current work, [22]
$CuSO_4$	125 g/m^3	\$2.165/kg	0.271 \$	Current work
$CoSO_4$	141 g/m^3	\$16.835/kg	2.374 \$	Current work
Electricity	5.5–60 (35) kWh/m^3	\$0.076/kWh	2.660 \$	[27–31]

3. Results and Discussions

3.1. Catalyst and Radical Effect

The degradation mechanism of dyes can generally be described in two main steps: the breakdown of the chromophore and the main skeleton of the dye structure, followed by mineralization of the degraded chromophore [32]. The color fading observed during treatment is typically a result of the degradation of the chromophore into smaller compounds, which is detected by the reduction in absorbance at the respective optimum wavelength for each dye. Subsequently, the smaller compounds produced due to chromophore degradation may undergo further deterioration into compounds with the lowest energy levels—carbon dioxide and water—known as mineralization, which is detected by a reduction in the concentration of TOC [33]. The typical dyes degradation mechanism, as explained, is shown in Figure 2 [12].

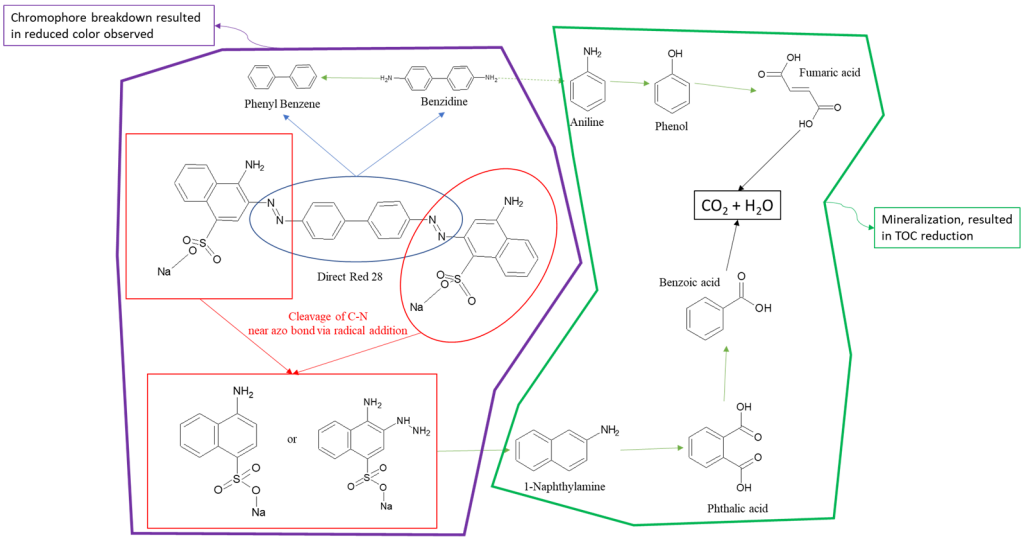

Figure 2. Possible dyes degradation mechanism, involving chromophore breakdown, followed by mineralization.

Degradation after 90 min of reaction is summarized in Table A1 and Figure A1 at Appendix A. The process is named by the combination of radical agent (H: H_2O_2, S: $K_2S_2O_8$), catalyst (Fe: $FeSO_4 \cdot 7H_2O$, Cu: $CuSO_4 \cdot 5H_2O$, Co: $CoSO_4 \cdot 7H_2O$) and pH (3, 7, 11). In the table, red text indicates the results with reduced performance, compared to processes without a catalyst at the same radical agent and pH.

For DR28, limited performance was observed in treatments with all catalyst–radical combinations, except with copper. The copper–PDS combination exhibited consistently good performance at all pH conditions, and exceptional results at pH 7 when paired with hydroxyl radicals (H-Cu-3). While there are limited references regarding DR28 degradation

using a copper-based Fenton process, previous research shows a high degradability of Cresol Red (CR) dyes using a copper–hydroxyl process [34].

The combination of iron–hydroxyl radicals (H-Fe-3, 7, 11) showed a poor performance, primarily due to the formation of sediment resulting from the complex reaction between iron and dye compounds. This finding is comparable with the finding from Bali et al. [35], that shows limited removal of DR28 via a photo-Fenton process. Previous research by Ay et al. [19] shows a high level of DR28 removal, up to 98%; however, the sample was centrifuged prior to analysis to remove the solid, which indicates sediment formation during the process.

Contrary to its performance on DR28, iron demonstrates superior efficacy on RB19 compared to other catalysts. At the same time, the performance of iron decreases with an increasing pH, similarly to DR28. Interestingly, the highest TOC removal was achieved with hydroxyl radicals at pH 3 (H-Fe-3); this was slightly lower than the 97.5% removal experiment by Bharadwaj and Saroha [36], and surpassing the PDS system at the same pH (S-Fe-3) by more than 30%. However, there was a plateau in removal after 30 min with the iron–hydroxyl radicals system, as shown in Figure 3, which became a recurring trend with other dyes as well. Copper also exhibits good TOC removal performance when paired with hydroxyl radicals at pH 3 (H-Cu-3), but is not effective under any other conditions. Finally, cobalt consistently underperforms in all situations.

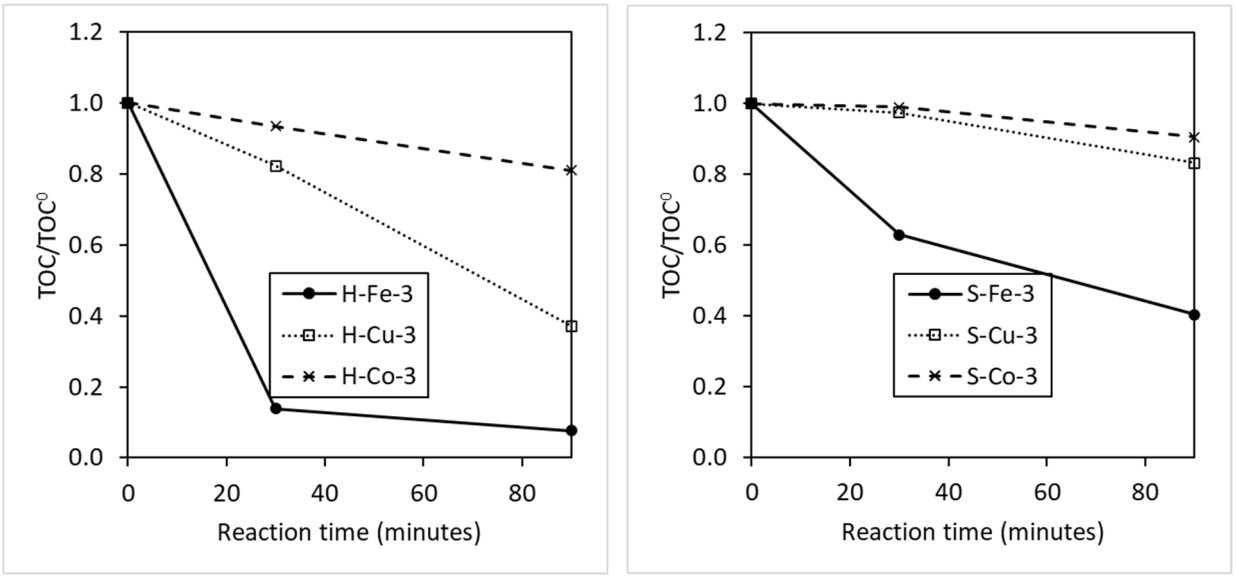

(**a**) (**b**)

Figure 3. Performance on RB19 using (**a**) hydroxyl (H) and (**b**) sulfate (S) radicals at pH 3 with an iron (Fe), copper (Cu), and cobalt (Co) catalyst combination.

All catalyst–radical combinations perform well on RBk5 for decolorization, except for the cobalt–hydroxyl radical combination at pH 11 (H-Co-11). A similar trend can be observed for TOC reduction. As can be seen in Figure 4, iron is able to degrade the dyes rapidly and it plateaus after the initial 30 min, while the other catalysts degrade more slowly but can achieve the same performance as iron after 90 min of operation. Cobalt performs unusually well on this dye, with the exception of the previously mentioned pH 11 hydroxyl–radical combination (H-Co-11), which had the highest 85% TOC reduction achieved at pH 3 with hydroxyl radicals (H-Co-3). Overall, cobalt only exhibits noticeable degradation capabilities with RBk5. This finding is similar to previous research, in which RBk5 can be degraded by various Fenton and Fenton-like methods [37].

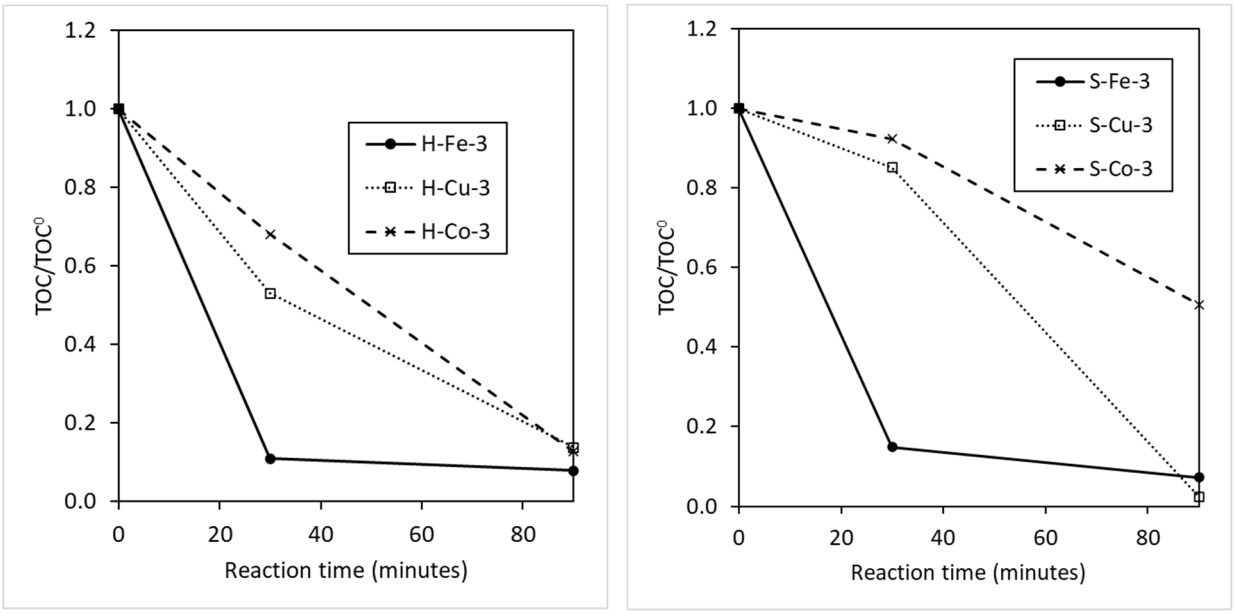

(**a**) (**b**)

Figure 4. Performance on RBk5 using (**a**) hydroxyl (H) and (**b**) sulfate (S) radicals at pH 3 with iron (Fe), copper (Cu), and cobalt (Co) catalyst combination.

3.2. Characteristics of Catalyst and Radical Agent

The first striking result is that for almost all catalyst–radical combinations, performance is almost always highest at pH 3. For instance, Figure 5 shows that at pH 3, complete decolorization of RB19 was achieved within the first 15 min of the reaction. On the other hand, at pH 11, the decolorization was slower and only reached 59% decolorization after 90 min. This is mostly attributed to the higher radical production under acidic conditions and the possible radical scavenging effect of carbonate species formed by the chemical degradation of dyes [8]. The more cationic state of dyes under acidic conditions also helps to improve their reactivity for degradation [38]. From our previous research [39], pH change may induce protonation to the dyes, make it more reactive in acidic situations, and enhancing the dyes' degradation. Under low pH conditions, hydrogen ions protonate amino groups bonded to a naphthyl ring, making them more vulnerable to radicals [40]. However, this phenomenon does not directly affect the chromophore, resulting in only an initial degradation reaction being affected. Since TOC reduction mainly occurs after the decolorization process, minimal changes in the main moieties lead to insignificant differences in TOC reduction between pH 3 and 7.

As one possible catalyst alternative, the poor performance of cobalt is quite surprising, but expected. Cobalt is actually considered to be more dominant than iron in the generation of sulfate radicals from peroxymonosulfate (PMS) [41,42], but such performance is not applicable to PDS. Moreover, cobalt has also previously been considered incapable of radical formation when introduced in a homogeneous situation, except when paired with PMS [42,43]. However, in this experiment, it is found that cobalt is still capable of producing radical ions which, in turn, degrade dyes, which is clearly reflected in RBk5, especially when combined with hydroxyl radicals.

As shown in Figure 6, cobalt could achieve comparable TOC reduction with other catalysts when applied to RBk5. On the other hand, cobalt performance on RB19 is much less pronounced than other catalysts. It is even clearer that the cobalt–hydroxyl radical combination could only achieve significant TOC removal when applied to RBk5 (Figure 7a), and its performance when paired with sulfate radicals is not as prominent as when paired with hydroxyl radicals. The combination of cobalt and peroxide forms a weak peroxy

radical (•OOH), rather than the strong hydroxyl radical [44]. The tendency to produce peroxy radicals is investigated by Turrà et al. [45], where hydroxyl radicals produced from Co^{2+} deperoxidation reactions will attack the available peroxide to produce weaker peroxy radicals, following Equations (1) and (2). This situation leads to more peroxyl radicals being available in the system, rather than hydroxyl radicals. Considering that peroxy radicals are much less reactive than hydroxyl radical by more than ten-fold, lower dye degradation performance is expected [46].

$$Co^{II} + H_2O_2 \rightarrow Co^{III} - OH + OH^{\bullet} \quad (1)$$

$$OH^{\bullet} + H_2O_2 \rightarrow H_2O + OOH^{\bullet} \quad (2)$$

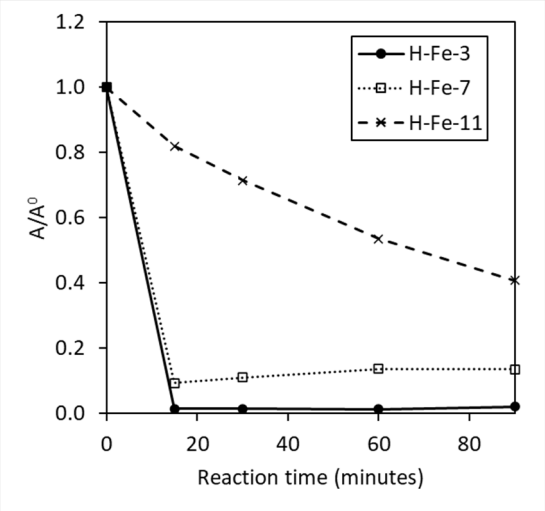

Figure 5. Decolorization performance of RB19 using an iron–peroxide combination (H-Fe) at various pHs.

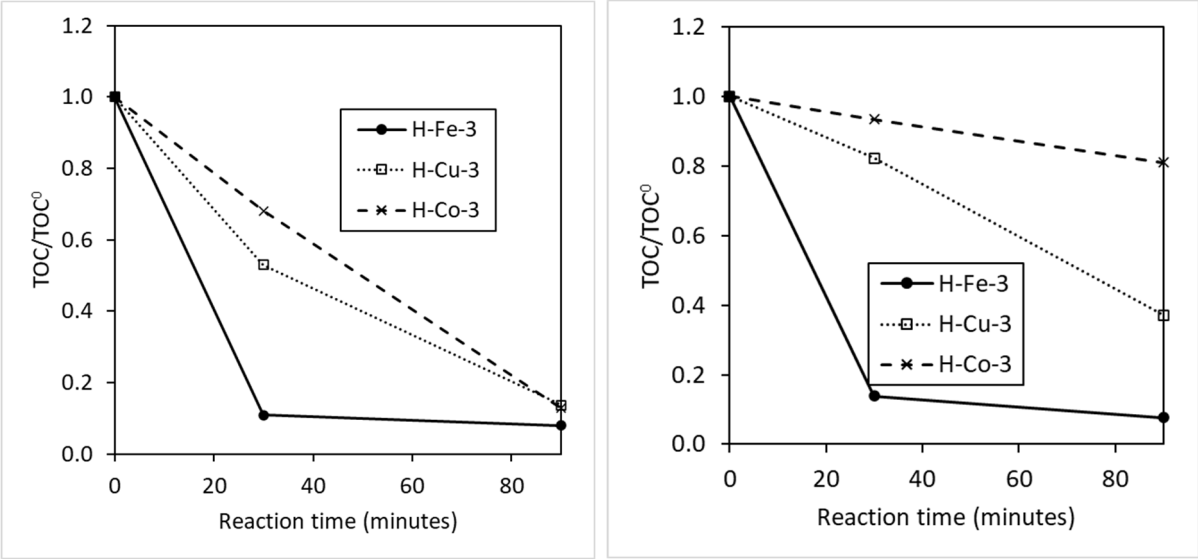

Figure 6. TOC reduction of (**a**) RBk5 and (**b**) RB19 with hydroxyl radical (H) at pH 3 with iron (Fe), copper (Cu), and cobalt (Co) catalyst combination.

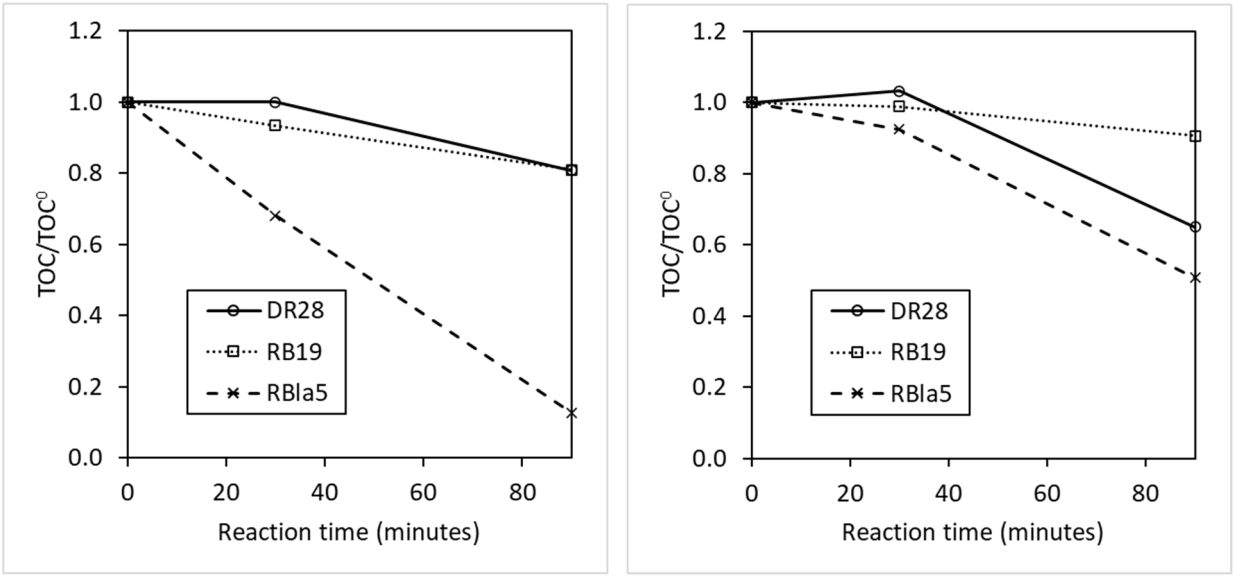

Figure 7. TOC reduction of cobalt (Co) paired with (**a**) hydroxyl and (**b**) sulfate radicals on various dyes.

This explains why noticeable degradation was only detected on RBk5, as the azo compound is much easier to degrade compared to the anthraquinone present in RB19. More sulfonate compounds (four in RBk5, compared to two in RB19) also play a role in the degradation of the side chain of the dyes by weak peroxy radicals. Due to those characteristics, we can classify RBk5 as an easy-to-degrade dye, especially compared to other dyes used in this experiment. Finally, it has been shown that cobalt has rather limited applicability and may not work properly with a wide array of dyes.

The plateauing performance of iron has always been imminent in many cases, and is often attributed to the non-thermodynamically favorable catalyst regeneration ($Fe^{3+} \rightarrow Fe^{2+}$, $E = -0.724$ V), which leads to less catalysts being available to activate the radical source [47,48]. However, this situation should be remedied by adding a UV lamp to provide the energy required to regenerate the spent catalyst. What is rarely mentioned, however, is the tendency of iron to form complexes with the dye compound and the by-product of the dye degradation process in a reaction known as mordanting [49,50]. This reaction leads to sedimentation in the solution and prevents mineralization. Furthermore, the low solubility of iron (both Fe(III) and Fe(II)) at a higher pH can also further promote the sediment formation, and also reduce the overall efficiency of the process [51]. Sediment formation has a significant effect, particularly on TOC reading, since removing the sediment using 0.45 µm filter leads to drastic TOC reduction, as indicated in Figure A2, and it is also possible that the majority of the organic content in a water sample is deposited in the sediment [52].

Sulfate radicals have been investigated as a possible improvement over hydroxyl radicals. Various research has shown the higher redox capabilities of the sulfate radical compared to the hydroxyl radical [53,54]. Sulfate radicals also have a longer half-life than hydroxyl radicals, which improves the contact time between the radical and the pollutant [55]. Another point that is believed to establish the sulfate radical as a better radical than the hydroxyl radical is the reaction selectivity, where the sulfate radical could efficiently react with organic compounds containing unsaturated bonds via electron transfer [56]. It is also found that in lower pH, sulfate radicals tend to be more prominent [57]. Combined with the protonated state of the dyes that makes the dye become more reactive [39], higher

removal efficiency is achieved. Meanwhile, at a higher pH, sulfate radicals tend to be converted into hydroxyl radicals [58] that has lower redox capabilities; thus, they have a lower performance.

On the other hand, the hydroxyl radical is a non-selective radical that can react with diverse compounds via hydrogen abstraction or electron addition [59]. An important point to note is that, due to their non-selective behavior, hydroxyl radicals could work as efficiently or perhaps even better than sulfate radicals under certain conditions [60,61]. Another possible reason is the fact that despite sulfate radicals having higher redox potential, hydrogen peroxide as a compound itself has a lower energy of the Lowest Unoccupied Molecular Orbital (LUMO) than PDS, which means that peroxide accepts electrons more easily than PDS, leading to easier activation [60]. With longer reaction times, the difference becomes negligible and ultimately depends on the redox capabilities of the radical [8].

Another unique finding was the difference in how the iron interacted with the treatment residue. As can be seen in Figure 8, there are apparent particulate species in both the sulfate and hydroxyl radicals that employed iron. However, the nature of the species was slightly different. The particulates formed after the UVPSFe treatment are finer than those formed after PF. The particulates in the UVPSFe system were almost like dissolved species and were only detected after filtration, whereas those in the PF system were more obvious. This could be attributed to the side product formed after treatment and its interaction with the iron species. However, further investigation and study is required to identify this matter.

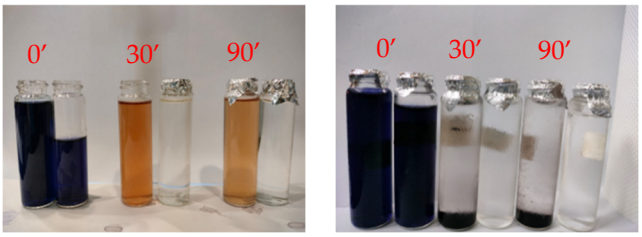

(**a**) (**b**)

Figure 8. Different particulate characteristics on DR28 treated with (**a**) sulfate and (**b**) hydroxyl radicals paired with iron catalyst at pH 3.

Finally, an interesting finding from sulfate radicals is that decolorization can occur even without additional external energy. This is not the case for peroxide, where no change in absorbance is observed in the peroxide-only system without the addition of an external force to decompose peroxide to a hydroxyl radical. This is further supported by the finding that there is a pH change in the PDS, both with and without a UV lamp. The pH changes occurred due to the conversion of sulfate radicals to hydroxyl radicals in the aqueous solution (Equation (3)). It was found that the heat could be one possible activator for sulfate radicals, and it can even be activated at a low temperature (20 ± 1 °C) at pH 7 [62], although it is not applicable to acidic conditions. This finding also aligns with other research, indicating that sulfate radicals are easier to activate under neutral conditions [8,56].

$$SO_4^{\bullet -} + H_2O \rightarrow SO_4^{2-} + OH^{\bullet} + H^+ \quad (3)$$

While the TOC reduction may still require further investigation, it at least indicates that the PDS system is much easier to implement compared to the peroxide system, although the acidic condition of the effluent will require further attention in the industrial application.

3.3. Cost Consideration for Technology Selection

Cost consideration was performed by calculating the cost associated with the most optimal result for each catalyst–radical combination. The variation in the price is compensated for via sensitivity analysis by varying the price of catalysts, radicals, and electricity (Figure A3). These references for the cost for calculation are shown in Table 1, which were then used to calculate the total costs outlined in Table 2 for Reactive Black 5, representing easily degradable dyes, and in Table 3 for Direct Red 28, representing recalcitrant dyes. It is important to note, however, that the change in electricity price can affect the overall cost of the process. As shown in Figure A3c, increasing the electricity price by 20% may increase the cost per TOC removed up to 14.7% in a process employing hydrogen peroxide.

Table 2. Cost comparison for reactive black 5.

Method	Cost ($/m^3)	TOC Removed		Cost Per TOC Removed ($/g)	Cost Per 90% TOC Removed ($)
		mg/L	%		
Fe-H	3.764	21.69	92.05	0.174	2.944
Cu-H	3.893	20.19	86.26	0.193	4.527
Co-H	5.996	19.77	87.24	0.303	7.004
Peroxide only	3.622	20.37	73.70	0.340	6.192
Fe-PDS	7.672	22.54	93.85	0.347	5.812
Cu-PDS	7.801	22.47	98.50	0.859	4.686
Co-PDS	9.904	11.53	49.27	0.178	36.161
PDS only	7.530	20.14	89.70	0.374	8.184

Table 3. Cost comparison for direct red 28.

Method	Cost ($/m^3)	TOC Removed		Cost Per TOC Removed ($/g)	Cost Per 90% TOC Removed ($)
		mg/L	%		
Fe-H	3.764	0.45	1.85	8.365	962.625
Cu-H	3.893	13.59	53.42	0.286	12.755
Co-H	5.996	5.70	21.41	1.052	63.787
Peroxide only	3.622	10.51	41.09	0.345	15.965
Fe-PDS	7.672	13.46	52.74	0.570	22.744
Cu-PDS	7.801	21.02	85.19	0.371	10.337
Co-PDS	9.904	9.76	39.77	1.015	50.662
PDS only	7.530	18.78	71.28	0.401	15.156

In general, the cost of the Fenton-based process stems from the consumption of electricity and chemicals. Electricity is primarily used for UV lamps, while chemicals include the radical agent and the catalyst. Other chemicals such as sulfuric acid or sodium hydroxide are typically used for pH adjustment, although their usage is not as significant as the main chemicals. Cost comparisons can be made on the basis of the volume of water treated, the number of organic compounds removed, or cost per order. The latter entails the expenditure required to reduce contaminants by one order of magnitude (achieving a 90% reduction) in a unit volume of water. While the first two components are easier to understand, the latter metric is more useful for evaluating different processes against a standardized criterion, especially in cases in which satisfactory performance is difficult to achieve [25].

As shown, the standard photo-Fenton process employing iron–peroxide emerges as the most cost-effective method, closely followed by copper–peroxide. Despite the higher performance of peroxydisulfate (PDS), its substantial consumption and higher unit cost limits its viability as a replacement for peroxide. Some other studies also find out the secondary contamination of treated water with inorganic sulfates that further limit the persulfate-based AOPs [63]. However, it is worth noting that the results in Table 2 are based on performance with relatively easy-to-degrade dyes (Reactive Black 5). When applied to recalcitrant dyes such as Direct Red 28 (Table 3), the performance of iron–peroxide deteriorates significantly due to complex reactions between iron and dye compounds, resulting in sedimentation [49]. In this scenario, copper demonstrates a significantly better performance, as it can still reduce 50% of the TOC in the system, compared to almost zero reduction when using iron. PDS also exhibits a relatively stable performance across different dyes and metals. However, given its high cost, justifying the use of PDS over peroxide requires a clear understanding of the characteristics of the dyes to be treated.

It is also interesting to note that the UV-peroxide process is promising in terms of cost-effectiveness. This system reliably removes color from easy-to-degrade dyes and boasts admirable TOC removal performance. Even with recalcitrant dyes, this process can still achieve good removal because there is no metal involved to cause complex reactions, although its performance remains below that of copper. Furthermore, the performance of this system does not decrease significantly at higher operating scales [64].

In summary, it is evident that the standard photo-Fenton process is highly cost-effective when used to treat easy-to-degrade dyes. Conversely, the presence of iron becomes an issue when treating recalcitrant dyes, making copper a more viable treatment option. Opting for copper as a catalyst is a prudent choice, especially when considering the wide range of dyes found in actual textile wastewater. However, in the worst-case scenario, as in all dyes are easily degraded, the cost can increase by around 60% per order of magnitude compared to when using iron as a catalyst. However, the cost of this process is highly sensitive to the change in the price of the radical, as indicated in Figure A3b.

However, it is important to note that the degradation behavior may differ on actual textile wastewater. In the actual textile wastewater, there are multiple variations that may affect the Fenton performance. For instance, actual textile wastewater may contain inorganic salts such as sodium sulfate or sodium chloride, that are commonly used in the dyeing process to promote color adsorption [65]. The existence of salt in the wastewater may reduce the overall performance of the Fenton process, specifically hindering the radical production via catalyst activation [66]. While color removal usually occurs in the last process in actual textile wastewater treatment in the industry, causing the salt content in the wastewater to typically already be quite low, understanding of the particular parameter effect on the process performance is still beneficial to project the actual cost required to achieve the desired color and organic removal from the wastewater.

4. Conclusions

This study investigates the application of Fenton-based processes for the degradation of textile dyes, focusing on Direct Red 28 (DR28), Reactive Blue 19 (RB19), and Reactive Black 5 (RBk5). The results highlight the importance of catalyst–radical combinations and pH conditions in influencing degradation efficiency. Copper and peroxydisulfate (PDS) exhibit consistent performances, with notable effectiveness in degrading RBk5. Iron, effective on RB19, has limitations on DR28, attributed to sediment formation and mordanting reactions. Finally, cobalt is incapable of properly degrading dyes, except with RBk5 under specific conditions.

Cost considerations highlight the standard photo-Fenton process (iron–peroxide) as being cost effective for easy-to-degrade dyes. However, copper is emerging as a more viable option for recalcitrant dyes, offering a superior performance at a reasonable cost. The UV-peroxide process is promising, especially for easy-to-degrade dyes, providing an economically competitive alternative.

In summary, this research improves the understanding of catalyst–radical interactions and their impact on dye degradation. The results will guide the selection of cost-effective technologies for textile wastewater treatment, taking into account the diverse nature of dye pollutants.

Author Contributions: Funding Acquisition, H.S.; Investigation, G.A.I.; Methodology, G.A.I.; Supervision, H.S.; Writing—original draft, G.A.I.; Writing—review and editing, H.S. All authors have read and agreed to the published version of the manuscript.

Funding: This research was funded by JSPS KAKENHI Grant Number JP22H01629.

Data Availability Statement: The data supporting this article is available upon request.

Conflicts of Interest: The authors declare no conflicts of interest.

Abbreviations

The following abbreviations are used in this manuscript:

DR28	Direct Red 28
RB19	Reactive Blue 19
RBk5	Reactive Black 5
TOC	Total Organic Carbon
PDS	Peroxydisulfate

Appendix A

Table A1. Summary of degradation results after 90 min.

Process	Decolorization			TOC Removal		
	DR28	**RB19**	**RBk5**	**DR28**	**RB19**	**RBk5**
H-Fe-3	49.05% ± 2.03%	97.89%	99.74%	3.47%	92.33%	92.05%
H-Cu-3	65.22% ± 5.65%	76.29%	99.86%	18.99%	62.90%	86.26%
H-Co-3	50.97%	76.73%	100.00%	19.10%	18.97%	87.24%
H-3	70.72%	81.55%	100.00%	41.09%	26.26%	73.70%
H-Fe-7	60.33%	86.43%	95.15%	1.59%	75.05%	87.32%
H-Cu-7	86.53%	47.09%	100.00%	53.42%	15.01%	80.05%
H-Co-7	76.29%	40.25%	99.88%	21.41%	7.52%	61.47%
H-7	78.58%	38.23%	100.00%	33.15%	13.25%	51.70%
H-Fe-11	58.76%	59.12%	98.61%	1.85%	49.66%	61.57%
H-Cu-11	81.61%	42.38%	97.29%	1.27%	26.31%	31.56%
H-Co-11	36.94%	10.15%	34.50%	0.82%	26.17%	1.74%
H-11	73.74%	61.68%	99.81%	10.53%	9.61%	55.98%
S-Fe-3	88.63% ± 4.87%	98.49%	100.00%	52.74%	59.60%	92.80%
S-Cu-3	98.48% ± 1.31%	99.07%	100.00%	72.32%	16.77%	97.53%
S-Co-3	95.93%	99.30%	100.00%	35.01%	9.43%	49.27%
S-3	92.52%	96.98%	99.83%	67.51%	27.39%	88.73%

Table A1. *Cont.*

Process	Decolorization			TOC Removal		
	DR28	RB19	RBk5	DR28	RB19	RBk5
S-Fe-7	90.77%	99.46%	100.00%	51.35%	65.27%	92.43%
S-Cu-7	96.88%	99.70%	100.00%	73.73%	17.83%	98.26%
S-Co-7	92.31%	99.67%	99.76%	24.30%	9.42%	44.86%
S-7	93.02%	97.14%	99.79%	70.46%	20.27%	89.70%
S-Fe-11	86.61%	99.36%	99.86%	40.72%	47.32%	93.85%
S-Cu-11	97.59%	99.36%	99.89%	85.19%	16.35%	98.50%
S-Co-11	94.63%	99.11%	99.71%	39.77%	14.70%	38.99%
S-11	95.15%	97.12%	99.79%	71.28%	22.93%	83.76%

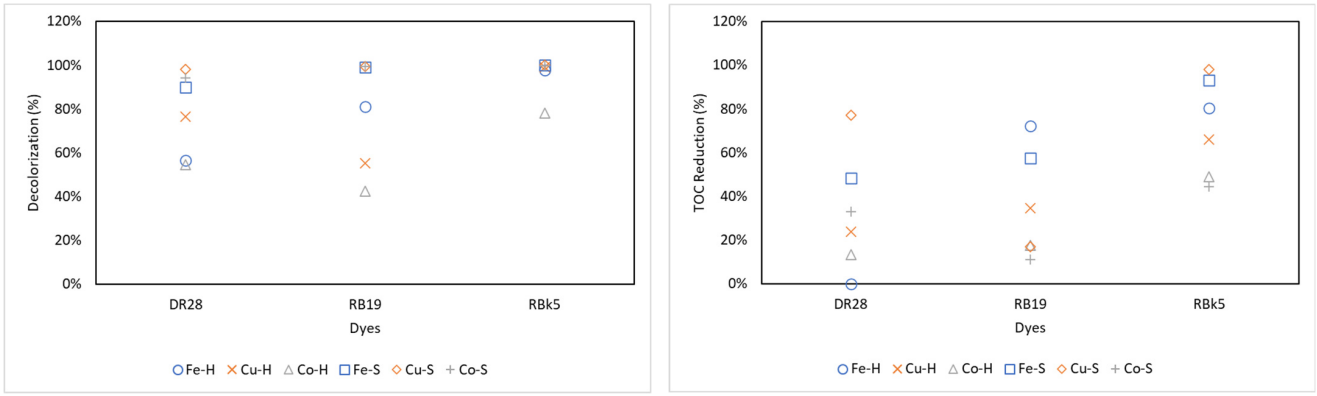

(**a**) (**b**)

Figure A1. Visualized summary of (**a**) decolorization and (**b**) TOC reduction of each catalyst and radical combination on different dyes.

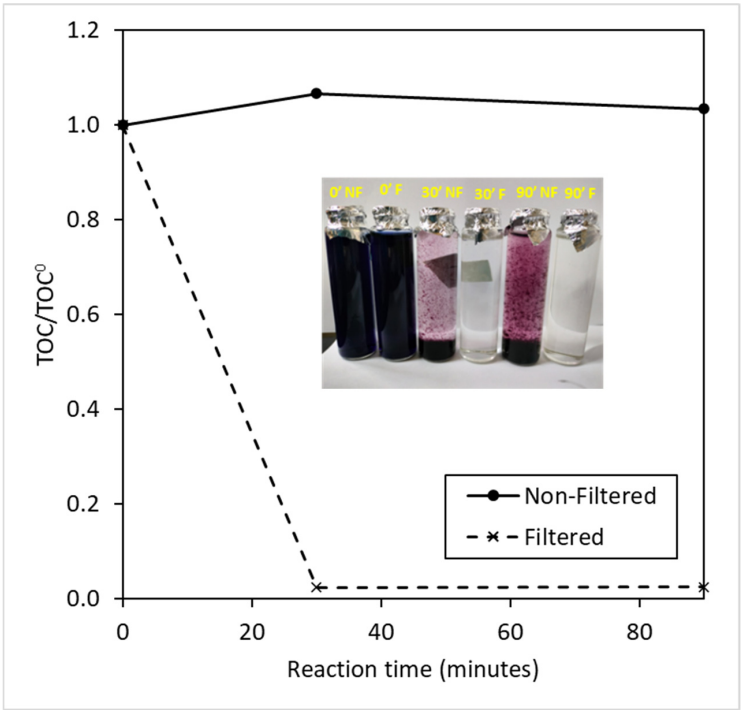

Figure A2. TOC reduction comparison of between filtered (dashed line) and non-filtered (straight line) DR28 treated with Fe-H at pH 3, showing drastic difference in TOC result, as also indicated by removal of solid and color between filtered (F) and non-filtered (NF) sample.

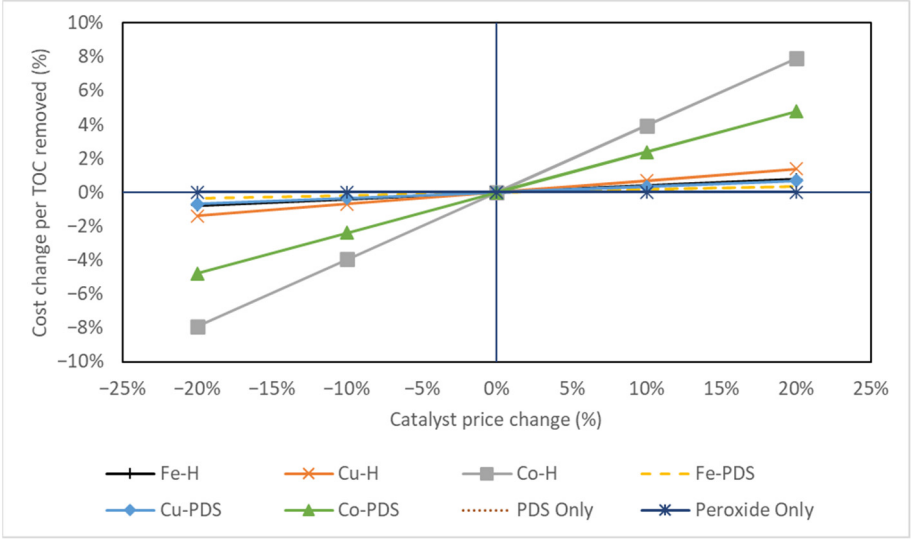

(**a**)

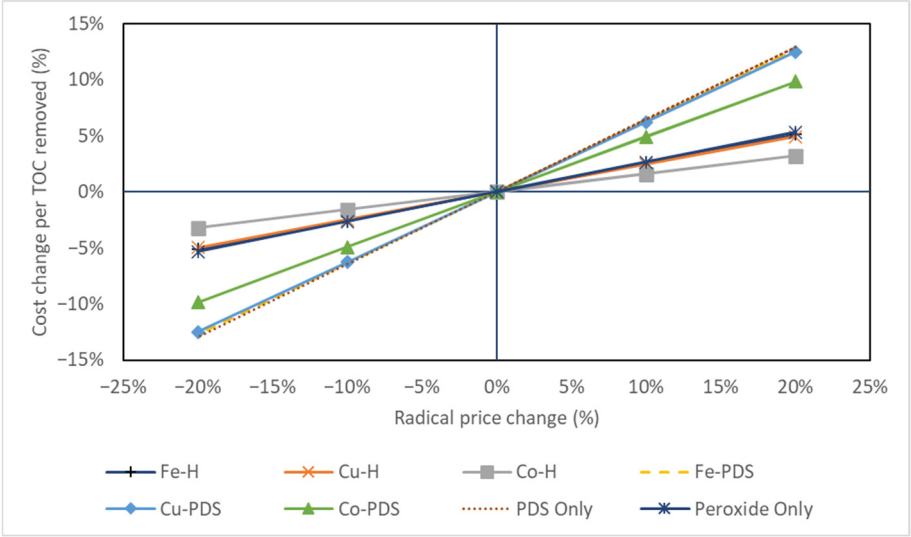

(**b**)

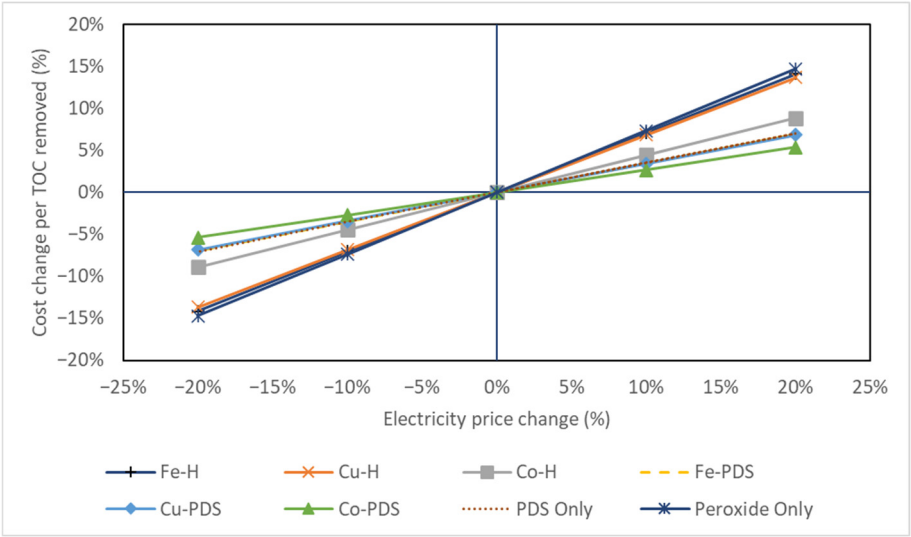

(**c**)

Figure A3. Sensitivity analysis for cost per TOC removed as function of (**a**) catalyst price change, (**b**) radical price change, and (**c**) electricity price change. A–a.

References

1. West, A.O.; Nolan, J.M.; Scott, J.T. Optical water quality and human perceptions of rivers: An ethnohydrology study. *Ecosyst. Health Sustain.* **2016**, *2*, e01230. [CrossRef]
2. Ovalle, R. A History of the Fenton Reactions (Fenton Chemistry for Beginners). In *Reactive Oxygen Species*; Ahmad, R., Ed.; IntechOpen: Rijeka, Croatia, 2022.
3. Cardona, Y.; Węgrzyn, A.; Miśkowiec, P.; Korili, S.A.; Gil, A. Heterogeneous Fenton- and photo-Fenton-like catalytic degradation of emerging pollutants using Fe_2O_3/TiO_2/pillared clays synthesized from aluminum industrial wastes. *J. Water Process Eng.* **2023**, *52*, 103494. [CrossRef]
4. Ramos, M.D.N.; Santana, C.S.; Velloso, C.C.V.; da Silva, A.H.M.; Magalhães, F.; Aguiar, A. A review on the treatment of textile industry effluents through Fenton processes. *Process Saf. Environ. Prot.* **2021**, *155*, 366–386. [CrossRef]
5. Ghaly, A.E.; Ananthashankar, R.; Alhattab, M.; Vasudevan Ramakrishnan, V. Production, characterization and treatment of textile effluents: A critical review. *J. Chem. Eng. Process Technol.* **2014**, *5*, 1–19.
6. Ismail, G.A.; Sakai, H. Review on effect of different type of dyes on advanced oxidation processes (AOPs) for textile color removal. *Chemosphere* **2021**, *291*, 132906. [CrossRef]
7. ZDHC Foundation. ZDHC Programme Textile Industry Wastewater Quality Guideline Literature Review—Revison 1. 2016. Available online: https://uploads-ssl.webflow.com/5c4065f2d6b53e08a1b03de7/5db6f553d5d32793e8e9a653_WastewaterQualityGuidelineLitReview.pdf. (accessed on 1 June 2025).
8. Ding, X.; Gutierrez, L.; Croue, J.P.; Li, M.; Wang, L.; Wang, Y. Hydroxyl and sulfate radical-based oxidation of RhB dye in UV/H_2O_2 and UV/persulfate systems: Kinetics, mechanisms, and comparison. *Chemosphere* **2020**, *253*, 126655. [CrossRef]
9. Yue, S.; Ye, W.; Xu, Z. SERS monitoring of the Fenton degradation reaction based on microfluidic droplets and alginate microparticles. *Analyst* **2019**, *144*, 5882–5889. [CrossRef]
10. Soares, P.A.; Souza, R.; Soler, J.; Silva, T.F.C.V.; Souza, S.M.A.G.U.; Boaventura, R.A.R.; Vilar, V.J.P. Remediation of a synthetic textile wastewater from polyester-cotton dyeing combining biological and photochemical oxidation processes. *Sep. Purif. Technol.* **2017**, *172*, 450–462. [CrossRef]
11. Sharma, S.; Kapoor, S.; Christian, R.A. Effect of Fenton process on treatment of simulated textile wastewater: Optimization using response surface methodology. *Int. J. Environ. Sci. Technol.* **2017**, *14*, 1665–1678. [CrossRef]
12. Ismail, G.A.; Sakai, H. Toxicity changes of dye degradation via photo-fenton treatment and the possible degradation mechanism. *Case Stud. Chem. Environ. Eng.* **2024**, *9*, 100665. [CrossRef]
13. Sponza, D.T.; Işik, M. Toxicity and intermediates of C.I. Direct Red 28 dye through sequential anaerobic/aerobic treatment. *Process Biochem.* **2005**, *40*, 2735–2744. [CrossRef]
14. Yakupova, E.I.; Bobyleva, L.G.; Vikhlyantsev, I.M.; Bobylev, A.G. Congo Red and amyloids: History and relationship. *Biosci. Rep.* **2019**, *39*, BSR20181415. [CrossRef]
15. El Bouraie, M.; El Din, W.S. Biodegradation of Reactive Black 5 by Aeromonas hydrophila strain isolated from dye-contaminated textile wastewater. *Sustain. Environ. Res.* **2016**, *26*, 209–216. [CrossRef]
16. Siddique, M.; Farooq, R.; Khan, Z.M.; Khan, Z.; Shaukat, S.F. Enhanced decomposition of reactive blue 19 dye in ultrasound assisted electrochemical reactor. *Ultrason. Sonochem.* **2011**, *18*, 190–196. [CrossRef]
17. Arslan, S.; Eyvaz, M.; Gürbulak, E.; Yüksel, E. A Review of State-of-the-Art Technologies in Dye-Containing Wastewater Treatment—The Textile Industry Case. In *Textile Wastewater Treatment*; IntechOpen: London, UK, 2016; pp. 1–28.
18. Fortunato, L.; Elcik, H.; Blankert, B.; Ghaffour, N.; Vrouwenvelder, J. Textile dye wastewater treatment by direct contact membrane distillation: Membrane performance and detailed fouling analysis. *J. Memb. Sci.* **2021**, *636*, 119552. [CrossRef]
19. Ay, F.; Catalkaya, E.C.; Kargi, F. A statistical experiment design approach for advanced oxidation of Direct Red azo-dye by photo-Fenton treatment. *J. Hazard. Mater.* **2009**, *162*, 230–236. [CrossRef] [PubMed]
20. Rehman, F.; Sayed, M.; Khan, J.A.; Shah, L.A.; Shah, N.S.; Khan, H.M.; Khattak, R. Degradation of crystal violet dye by fenton and photo-fenton oxidation processes. *Z. Fur Phys. Chem.* **2018**, *232*, 1771–1786. [CrossRef]
21. Bidu, J.M.; Njau, K.N.; Rwiza, M.; Van der Bruggen, B. Textile wastewater treatment in anaerobic reactor: Influence of domestic wastewater as co-substrate in color and COD removal. *S. Afr. J. Chem. Eng.* **2023**, *43*, 112–121. [CrossRef]
22. Çalık, Ç.; Çifçi, D.İ. Comparison of kinetics and costs of Fenton and photo-Fenton processes used for the treatment of a textile industry wastewater. *J. Environ. Manage.* **2022**, *304*, 114234. [CrossRef]
23. Ribeiro, J.P.; Marques, C.C.; Portugal, I.; Nunes, M.I. Fenton processes for AOX removal from a kraft pulp bleaching industrial wastewater: Optimisation of operating conditions and cost assessment. *J. Environ. Chem. Eng.* **2020**, *8*, 104032. [CrossRef]
24. Varank, G.; Guvenc, S.Y.; Çebi, A.; Güven, E.C. Central composite design for the advanced treatment of biologically treated leachate nanofiltration concentrate using zero-valent copper and iron activated persulfate. *Desalin. Water Treat.* **2020**, *208*, 434–447. [CrossRef]
25. Liu, K.; Roddick, F.A.; Fan, L. Impact of salinity and pH on the UVC/H_2O_2 treatment of reverse osmosis concentrate produced from municipal wastewater reclamation. *Water Res.* **2012**, *46*, 3229–3239. [CrossRef]

26. Baresel, C.; Harding, M.; Junestedt, C. Removal of Pharmaceutical Residues from Municipal Wastewater Using UV/H2O2. 2019. Available online: https://urn.kb.se/resolve?urn=urn:nbn:se:ivl:diva-2828 (accessed on 15 June 2025).
27. Rueda-Márquez, J.J.; Levchuk, I.; Manzano, M.; Sillanpää, M. Toxicity reduction of industrial and municipal wastewater by advanced oxidation processes (Photo-fenton, UVC/H_2O_2, electro-fenton and galvanic fenton): A review. *Catalysts* **2020**, *10*, 612. [CrossRef]
28. EPA. Technologies and Costs Document for the Final Long Term 2 Enhanced Surface Water Treatment Rule and Final Stage 2 Disinfectants and Disinfection Byproducts Rule. 2005. Available online: https://nepis.epa.gov/Exe/ZyPURL.cgi?Dockey=P100LZ09.TXT (accessed on 15 June 2025).
29. Rueda-Márquez, J.J.; Pintado-Herrera, M.G.; Martín-Díaz, M.L.; Acevedo-Merino, A.; Manzano, M.A. Combined AOPs for potential wastewater reuse or safe discharge based on multi-barrier treatment (microfiltration-H_2O_2/UV-catalytic wet peroxide oxidation). *Chem. Eng. J.* **2015**, *270*, 80–90. [CrossRef]
30. Kajitvichyanukul, P.; Suntronvipart, N. Evaluation of biodegradability and oxidation degree of hospital wastewater using photo-Fenton process as the pretreatment method. *J. Hazard. Mater.* **2006**, *138*, 384–391. [CrossRef]
31. Umar, M.; Roddick, F.; Fan, L. Impact of coagulation as a pre-treatment for UVC/H_2O_2-biological activated carbon treatment of a municipal wastewater reverse osmosis concentrate. *Water Res.* **2016**, *88*, 12–19. [CrossRef]
32. Nacowong, P.; Saikrasun, S. Thermo-oxidative and weathering degradation affecting coloration performance of lac dye. *Fash. Text.* **2016**, *3*, 18. [CrossRef]
33. Ghoreishian, S.M.; Badii, K.; Norouzi, M.; Rashidi, A.; Montazer, M.; Sadeghi, M.; Vafaee, M. Decolorization and mineralization of an azo reactive dye using loaded nano-photocatalysts on spacer fabric: Kinetic study and operational factors. *J. Taiwan Inst. Chem. Eng.* **2014**, *45*, 2436–2446. [CrossRef]
34. Seraghni, N.; Dekkiche, B.A.; Debbache, N.; Belattar, S.; Mameri, Y.; Belaidi, S.; Sehili, T. Photodegradation of cresol red by a non-iron Fenton process under UV and sunlight irradiation: Effect of the copper(II)-organic acid complex activated by H_2O_2. *J. Photochem. Photobiol. A Chem.* **2021**, *420*, 113485. [CrossRef]
35. Bali, U.; Çatalkaya, E.; Şengül, F. Photodegradation of reactive black 5, direct red 28 and direct yellow 12 using UV, UV/H_2O_2 and UV/H_2O_2/Fe^{2+}: A comparative study. *J. Hazard. Mater.* **2004**, *114*, 159–166. [CrossRef]
36. Bharadwaj, A.; Saroha, A.K. Decolorization of the Textile Wastewater Containing Reactive Blue 19 Dye by Fenton and Photo-Fenton Oxidation. *J. Hazard. Toxic Radioact. Waste* **2015**, *19*, 4014043. [CrossRef]
37. Liu, X.; Qiu, M.; Huang, C. Degradation of the Reactive Black 5 by Fenton and Fenton-like system. *Procedia Eng.* **2011**, *15*, 4835–4840. [CrossRef]
38. Baeza, C.; Knappe, D.R.U. Transformation kinetics of biochemically active compounds in low-pressure UV Photolysis and UV/H_2O_2 advanced oxidation processes. *Water Res.* **2011**, *45*, 4531–4543. [CrossRef]
39. Ismail, G.A.; Sakai, H. pH-Dependent Dye Protonation and the Effect of Iron on Dye Degradation During Fenton-Based Processes. *Ozone Sci. Eng.* **2024**, *46*, 294–308. [CrossRef]
40. Mahmoud, A.S.; Ghaly, A.E.; Brooks, S.L. Influence of temperature and pH on the stability and colorimetric measurement of textile dyes. *Am. J. Biochem. Biotechnol.* **2007**, *3*, 33–41. [CrossRef]
41. Manos, D.; Miserli, K.; Konstantinou, I. Perovskite and spinel catalysts for sulfate radical-based advanced oxidation of organic pollutants in water and wastewater systems. *Catalysts* **2020**, *10*, 1299. [CrossRef]
42. Anipsitakis, G.P.; Dionysiou, D.D. Radical generation by the interaction of transition metals with common oxidants. *Environ. Sci. Technol.* **2004**, *38*, 3705–3712. [CrossRef]
43. Ding, Y.; Fu, L.; Peng, X.; Lei, M.; Wang, C.; Jiang, J. Copper catalysts for radical and nonradical persulfate based advanced oxidation processes: Certainties and uncertainties. *Chem. Eng. J.* **2022**, *427*, 131776. [CrossRef]
44. Kadiiska, M.B.; Maples, K.R.; Mason, R.P. A comparison of cobalt(II) and iron(II) hydroxyl and superoxide free radical formation. *Arch. Biochem. Biophys.* **1989**, *275*, 98–111. [CrossRef]
45. Turrà, N.; Neuenschwander, U.; Baiker, A.; Peeters, J.; Hermans, I. Mechanism of the catalytic deperoxidation of tert-butylhydroperoxide with cobalt(II) acetylacetonate. *Chem.—A Eur. J.* **2010**, *16*, 13226–13235. [CrossRef]
46. Kwon, D.Y.; Kim, S.J.; Lee, J.W.; Kim, Y.C. Comparison of hydroxyl radical, peroxyl radical, and peroxynitrite scavenging capacity of extracts and active components from selected medicinal plants. *Toxicol. Res.* **2013**, *26*, 321–327. [CrossRef]
47. Anipsitakis, G.P.; Dionysiou, D.D. Degradation of organic contaminants in water with sulfate radicals generated by the conjunction of peroxymonosulfate with cobalt. *Environ. Sci. Technol.* **2003**, *37*, 4790–4797. [CrossRef]
48. Antoniou, M.G.; Nicolaou, P.A.; Shoemaker, J.A.; de la Cruz, A.A.; Dionysiou, D.D. Impact of the morphological properties of thin TiO_2 photocatalytic films on the detoxification of water contaminated with the cyanotoxin, microcystin-LR. *Appl. Catal. B Environ.* **2009**, *91*, 165–173. [CrossRef]
49. Dutta, P.; Mahjebin, S.; Sufian, M.A.; Razaya Rabbi, M.; Chowdhury, S.; Imran, I.H. Impacts of natural and synthetic mordants on cotton knit fabric dyed with natural dye from onion skin in perspective of eco-friendly textile process. *Mater. Today Proc.* **2021**, *47*, 2633–2640. [CrossRef]

50. Vargas, S.; Santamaria-Holek, I.; Rodríguez, R. Photocurrent oscillations in natural dyes-based DSSCs with different mordant and assistants: Their role in oscillations and color stability. *Mater. Chem. Phys.* **2022**, *286*, 126163. [CrossRef]
51. Lee, H.; Lee, H.J.; Sedlak, D.L.; Lee, C. pH-Dependent reactivity of oxidants formed by iron and copper-catalyzed decomposition of hydrogen peroxide. *Chemosphere* **2013**, *92*, 652–658. [CrossRef]
52. Dianto, A.; Ridwansyah, I.; Subehi, L. Organic matter and organic carbon levels in sediments of Lake Maninjau, West Sumatra. *IOP Conf. Ser. Earth Environ. Sci.* **2020**, *535*, 012030. [CrossRef]
53. Xia, H.; Li, C.; Yang, G.; Shi, Z.; Jin, C.; He, W.; Xu, J.; Li, G. A review of microwave-assisted advanced oxidation processes for wastewater treatment. *Chemosphere* **2022**, *287*, 131981. [CrossRef] [PubMed]
54. Behnami, A.; Aghayani, E.; Benis, K.Z.; Sattari, M.; Pourakbar, M. Comparing the efficacy of various methods for sulfate radical generation for antibiotics degradation in synthetic wastewater: Degradation mechanism, kinetics study, and toxicity assessment. *RSC Adv.* **2022**, *12*, 14945–14956. [CrossRef] [PubMed]
55. Xia, X.; Zhu, F.; Li, J.; Yang, H.; Wei, L.; Li, Q.; Jiang, J.; Zhang, G.; Zhao, Q. A Review Study on Sulfate-Radical-Based Advanced Oxidation Processes for Domestic/Industrial Wastewater Treatment: Degradation, Efficiency, and Mechanism. *Front. Chem.* **2020**, *8*, 592056. [CrossRef]
56. Guerra-Rodríguez, S.; Rodríguez, E.; Singh, D.N.; Rodríguez-Chueca, J. Assessment of sulfate radical-based advanced oxidation processes for water and wastewater treatment: A review. *Water* **2018**, *10*, 1828. [CrossRef]
57. Ahmadi, M.; Ghanbari, F.; Moradi, M. Photocatalysis assisted by peroxymonosulfate and persulfate for benzotriazole degradation: Effect of ph on sulfate and hydroxyl radicals. *Water Sci. Technol.* **2015**, *72*, 2095–2102. [CrossRef] [PubMed]
58. Guan, Y.H.; Ma, J.; Li, X.C.; Fang, J.Y.; Chen, L.W. Influence of pH on the formation of sulfate and hydroxyl radicals in the UV/Peroxymonosulfate system. *Environ. Sci. Technol.* **2011**, *45*, 9308–9314. [CrossRef] [PubMed]
59. Zhao, Q.; Mao, Q.; Zhou, Y.; Wei, J.; Liu, X.; Yang, J.; Luo, L.; Zhang, J.; Chen, H.; Chen, H.; et al. Metal-free carbon materials-catalyzed sulfate radical-based advanced oxidation processes: A review on heterogeneous catalysts and applications. *Chemosphere* **2017**, *189*, 224–238. [CrossRef] [PubMed]
60. Antoniou, M.G.; de la Cruz, A.A.; Dionysiou, D.D. Degradation of microcystin-LR using sulfate radicals generated through photolysis, thermolysis and e^- transfer mechanisms. *Appl. Catal. B Environ.* **2010**, *96*, 290–298. [CrossRef]
61. Nawaz, T.; Sengupta, S. Chapter 13—Wastewater: Novel treatment technologies and source for epidemiological studies. In *Handbook of Water Purity and Quality*, 2nd ed.; Ahuja, E., Ed.; Academic Press: Amsterdam, The Netherlands, 2021; pp. 293–337.
62. Ji, Y.; Shi, Y.; Dong, W.; Wen, X.; Jiang, M.; Lu, J. Thermo-activated persulfate oxidation system for tetracycline antibiotics degradation in aqueous solution. *Chem. Eng. J.* **2016**, *298*, 225–233. [CrossRef]
63. Kamenická, B.; Weidlich, T. A Comparison of Different Reagents Applicable for Destroying Halogenated Anionic Textile Dye Mordant Blue 9 in Polluted Aqueous Streams. *Catalysts* **2023**, *13*, 460. [CrossRef]
64. De la Cruz, N.; Esquius, L.; Grandjean, D.; Magnet, A.; Tungler, A.; de Alencastro, L.F.; Pulgarín, C. Degradation of emergent contaminants by UV, UV/H_2O_2 and neutral photo-Fenton at pilot scale in a domestic wastewater treatment plant. *Water Res.* **2013**, *47*, 5836–5845. [CrossRef]
65. Yildirim, R.; Eskikaya, O.; Keskinler, B.; Karagunduz, A.; Dizge, N.; Balakrishnan, D. Fabric dyeing wastewater treatment and salt recovery using a pilot scale system consisted of graphite electrodes based on electrooxidation and nanofiltration. *Environ. Res.* **2023**, *234*, 116283. [CrossRef]
66. Bacardit, J.; Stötzner, J.; Chamarro, E.; Esplugas, S. Effect of salinity on the photo-fenton process. *Ind. Eng. Chem. Res.* **2007**, *46*, 7615–7619. [CrossRef]

Disclaimer/Publisher's Note: The statements, opinions and data contained in all publications are solely those of the individual author(s) and contributor(s) and not of MDPI and/or the editor(s). MDPI and/or the editor(s) disclaim responsibility for any injury to people or property resulting from any ideas, methods, instructions or products referred to in the content.